Original Article

Analysis of Human Papillomavirus-Associated Cervical Cancer Differentially Expressed Genes and Identification of Prognostic Factors using Integrated Bioinformatics Approaches

Saba Hatefi-Shogae, Modjtaba Emadi-Baygi, Rasoul Ghaedi-Heydari
Department of Genetics, Faculty of Basic Sciences, Shahrekord University, Shahrekord, Iran

Abstract

Background: Human papillomavirus (HPV)-induced cervical cancer progresses through a series of steps. Despite our limited understanding of the mechanisms driving this progression, identifying the key genes involved could significantly improve early detection and treatment.

Materials and Methods: Two gene expression profiles of GSE9750 and GSE6791, which included cervical cancer HPV-positive and -negative samples, were evaluated using the R limma package with established cut-off criteria of *P* value < 0.05 and | fold change| ≥ 1. KEGG pathway enrichment was performed to identify potential pathways. Weighted gene co-expression network analysis (WGCNA) was used to discover co-expressed gene modules and trait–module connections.

Results: Considering the defined criteria, 115 differentially expressed genes (DEGs) were identified. The DEG's KEGG pathway enrichment analysis revealed enrichment in highly relevant pathways to the HPV infection, including cell cycle, viral carcinogenesis, autophagy-animal, Epstein-Barr virus infection, human T-cell leukemia virus 1 infection, and microRNAs in cancer. WGCNA results in 13 co-expression modules, and the magenta module is identified with significant relations to HPV, cervical cancer stage, and metastasis traits. The survival analysis identified *BEX1* and *CDC45* as potential prognostic factors in HPV-associated cervical cancer.

Conclusion: The innovation of our work lies in identifying essential genes associated with the multi-step process of cervical carcinogenesis. In fact, the current study has the potential to give a distinct viewpoint on the molecular pathways linked to cervical cancer. Considering the potential importance of the hub genes, we recommend conducting in-depth wet lab research to determine their impact on the biological mechanisms of cervical cancer.

Keywords: *BEX1*, *CDC45*, cell cycle, cervical cancer, gene expression, gene modules, gene networks, HPV

Address for correspondence: Dr. Modjtaba Emadi-Baygi, Department of Genetics, Faculty of Basic Sciences, Shahrekord University, PO Box 115, Shahrekord, Iran.
E-mail: emadibaygi@gmail.com
Submitted: 05-Sep-2023; **Revised:** 05-Dec-2023; **Accepted:** 09-Dec-2023; **Published:** 23-Sep-2024

Introduction

Cervical cancer is the most prevalent kind of gynecological malignancy. Cervical malignant tumor incidence and death rates are fourth globally, behind only breast, colorectal, and lung cancer in females.[1] However, in developing nations, cervical cancer comes in second only to breast cancer in terms of incidence and death.[2] Cervical cancer is one of the cancers that may be avoided by being screened. Cervical cancer incidence is decreasing year by year as screening becomes conventional. However, since early cervical cancer has no signs, many individuals are detected in the middle or late stages of the disease.[3] Previous research has linked the development of cervical cancer to chronic infection with high-risk human papillomavirus (HPV).[4] High-risk HPVs infected more than

Access this article online
Quick Response Code:
Website: www.advbiores.net
DOI: 10.4103/abr.abr_338_23

How to cite this article: Hatefi-Shogae S, Emadi-Baygi M, Ghaedi-Heydari R. Analysis of human papillomavirus-associated cervical cancer differentially expressed genes and identification of prognostic factors using integrated bioinformatics approaches. Adv Biomed Res 2024;13:78.

99.7% of cervical cancer patients. The most common forms are HPV16 and HPV18 high-risk sub-types.[5] High-risk HPVs are responsible for the production of the oncoproteins E6 and E7 that target many more cellular factors including p53 and pRb. The E6 protein interacts with p53 protein, inducing p53 degradation and, as a result, interfering with cellular death. The E7 protein binds to pRB, inactivating it and changing cell cycle regulatory pathways. The E6 and E7 oncoproteins collectively have the ability to exert a global change allowing infected cells to alter genetically and epigenetically, causing cancer cells to progress.[6]

Because the most effective screening tests, the Pap test and the HPV test, are extensively utilized in the clinic for cervical cancer detection,[7] most individuals may be detected and treated at an early stage of cervical cancer development. There is currently no operative therapy for advanced or recurring cervical cancer.[8,9] Surgical procedures, radiation, and platinum-based adjuvant chemotherapy are the primary therapies for cervical cancer. Early-stage cervical cancer is mostly treated surgically, with a 5-year survival rate of 88–95%. However, a few treatment options are available for patients in the intermediate and advanced phases, and the therapeutic efficacy of radiation and chemotherapy is inadequate.[10-12] Consequently, it is essential to identify new molecular biomarkers, therapeutic targets, and prognostic assessment indices for cervical cancer. The widespread use of bioinformatics tools has aided in the development of novel cancer biomarkers.[13-16]

Recent research has focused on identifying differentially expressed genes (DEGs) while ignoring the complex networks of genes and the clinical symptoms associated with genes.[17] However, mounting data shows that the emergence of cervical cancer is caused by several aberrantly expressed genes.[18,19] Weighted gene co-expression network analysis (WGCNA), a high-throughput data mining tool, finds essential biological modules utilizing high-throughput gene expression data.[20] WGCNA has been widely employed in tumor marker studies in recent years. We used DEG expression profiles from the Gene Expression Omnibus (GEO) public database to establish a co-expression network to explore HPV-associated cervical cancer progression-related hub genes. These highlighted hub genes may be used to predict cervical cancer patients' 3- and/or 5-year survival rates. The potential relevance of these genes as biomarkers has to be investigated further, and it may also give a theoretical foundation for assessing the prognosis of cervical cancer patients.

Materials and Methods

Retrieving microarray data and analysis of DEGs

The GEO database (www.ncbi.nlm.nih.gov/geo) was used to retrieve gene expression profiles of cervical cancer by searching for terms such as "cervical cancer" and "HPV" or "human papillomavirus." GSE9750 (https://www.ncbi.nlm.nih.gov/geo/query/acc.cgi?acc = GSE9750) and GSE6791 (https://www.ncbi.nlm.nih.gov/geo/query/acc.cgi?acc = GSE6791) were the most eligible results with a sufficient sample size. The datasets are detailed in Table 1. R v4.0.5 (https://www.r-project.org/) was used to pre-process the raw expression data. The Robust Multi-Array Average (RMA) technique in Bioconductor's affy package (https://rdrr.io/bioc/affy/man/rma.html) was used to pre-process gene expression profile data, which included background correction, quantile normalization, and summarizing. These two datasets were merged, and batch effect removal was performed using the ComBat package (https://rdrr.io/bioc/sva/man/ComBat.html). To eliminate false positives and keep high expression levels of DEGs for downstream analysis, we only kept the expressed probes with the criterion of "present (P)" in more than 50% of all the samples for the datasets, which was found using the mas 5 calls function in the affy package.[21] The Linear Models for Microarray Data (limma) package was used to discover DEGs by comparing expression levels across groups. The cut-off criteria for DEGs were P value < 0.05 and | fold change (FC)| ≥1.[22]

Pathway enrichment analysis

The KEGG database is used to study the function and applications of biological systems based on genomics or molecular information.[23] In this investigation, the enrichKEGG functions in the software R package pathfinder were used to perform enrichment analysis and pathway analysis of the DEGs in order to discover the essential KEGG pathways ($P < 0.05$). The pathfindR program in R software was used to identify clustering across pathways based on the shared genes.[24]

WGCNA network construction

Gene co-expression networks were constructed using WGCNA, a system biology approach that translates co-expression data into connection weight or topological overlap metrics, in order to study the interactions between genes.[20] Co-expression analysis was often used to determine the association between gene expression levels. Genes with similar expression patterns are related to the same pathway or functional component.[25] As a consequence, constructing a gene co-expression network aids in the identification of genes with similar biological functions.[26] Three thousand DEGs with the most variance in the target datasets were selected for this research and utilized to build weighted co-expression modules in R using the WGCNA package. The pickSoftThreshold function was used to evaluate the mean connectivity and scale independence of networks with varying power levels, which selected as soft thresholding power $\beta = 4$. Using the minModuleSize function, the minimum number of genes in each module was considered 30.

Survival analysis

Survival analysis was used to assess the association between the expression levels of the hub genes and the prognosis of cervical cancer using Gene Expression Profiling Interactive Analysis (GEPIA). It is a database that uses The Cancer Genome Atlas (TCGA) data to assess gene survival outcomes.

Moreover, the GAPDH gene was utilized to normalize data from targeted genes.

Results

Identification of DEGs

This gene expression analysis aimed to find the DEGs with the most significant expression changes. 115 DEGs were discovered based on the given criteria; *P* value < 0.05 and | FC| ≥ 1, detailed in Supplementary Table 1. The top ten genes with the most altered expression levels are represented in Table 2. Figure 1 depicts a box plot for gene expression-related data after normalization to analyze data distribution as well as a volcano plot of DEGs in cervical cancer samples compared to controls.

Pathway enrichment analysis

KEGG pathway analysis showed that six significant enrichment pathways existed, including "Cell cycle", "Viral carcinogenesis", "Autophagy-animal", "Epstein-Barr virus infection", "Human T-cell leukemia virus 1 infection", and "MicroRNAs in cancer" [Figure 2a]. Clustering between pathways based on shared genes demonstrated notable clustering between the cell cycle, human T-cell leukemia virus 1 infection, viral carcinogenesis, cellular senescence, P53, and foxO signaling pathways [Figure 2b]. The viral carcinogenesis pathways of viruses including HBV, HCV, EBV, HPV, HTLV-1, and KSHV are illustrated in Figure 3, and the involvement of cell cycle in the HPV carcinogenesis is specified.

Construction of WGCNA and identification of desired modules

The WGCNA package was used in this study to build co-expression modules on the GSE9750 and GSE6791 expression profiles [Figure 4a]. Graphs of scale

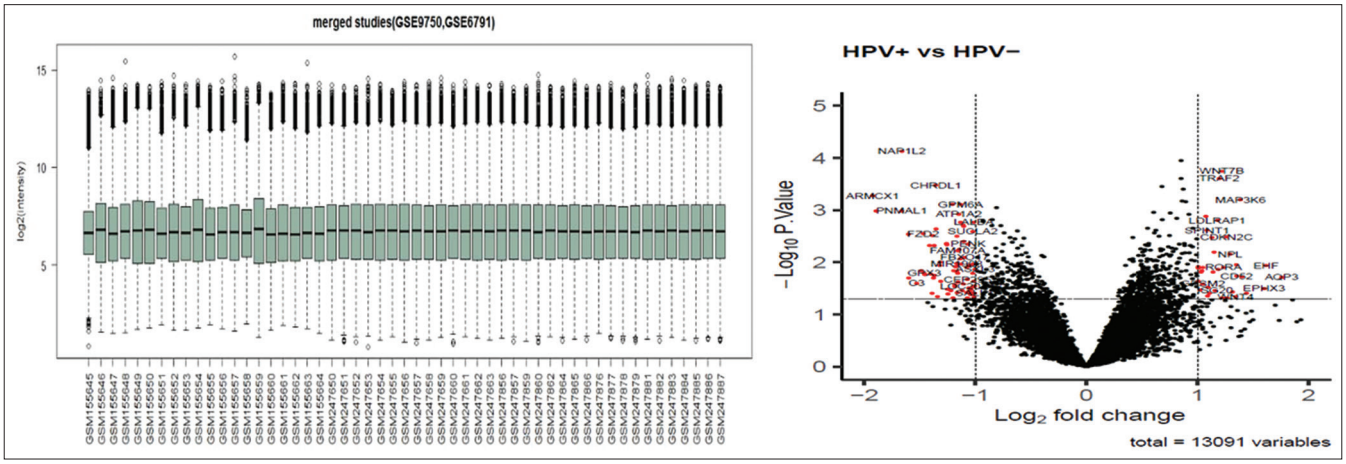

Figure 1: The boxplot of datasets and DEGs' volcano plan. Screening for DEGs was done using a *P* value < 0.05 and | FC| ≥ 1

Table 1: Details of cervical cancer microarray datasets

GEO accession	Type of samples	Sample count	Platforms	Assessed on	Accessible link
GSE9750	Cervix epithelium	31 (HPV +) 3 (HPV -)	GPL96 (Affymetrix Human Genome U133A Array)	February 26, 2020	https://www.ncbi.nlm.nih.gov/geo/query/acc.cgi?acc=GSE9750
GSE6791	Cervix epithelium	17 (HPV +) 3 (HPV -)	GPL570 (Affymetrix Human Genome U133 Plus 2.0 Array)	February 26, 2020	https://www.ncbi.nlm.nih.gov/geo/query/acc.cgi?acc=GSE6791

Table 2: Top ten DEGs in HPV-associated cervical cancer

Gene name	logFC	AveExpr	*t*	*P*	adj.*P*	B
KRT15	3.393497576	10.75089062	2.832760285	0.006417107	0.87125001	-2.795995092
CDH13	-2.25219	5.382494	-3.77544	0.00039	0.578434	-1.29513
SYNGR3	2.114242367	7.419139949	3.67614096	0.000534734	0.640594986	-1.463170267
ARMCX1	-1.92488	6.132086	-3.67404	0.000538	0.640595	-1.4667
CYTL1	-1.89299	4.244747	-3.46308	0.001035	0.695686	-1.8169
AQP3	1.755985	9.585711	2.408208	0.019374	0.87125	-3.38387
PNMAL1	-1.66416996	5.424176411	-3.460990132	0.001041616	0.695685945	-1.820315347
NAP1L2	-1.661284382	4.261195898	-4.282099081	7.39E-05	0.578433778	-0.412262713
EHF	1.615501	7.507107	2.609951	0.011615	0.87125	-3.11272
ANXA10	-1.598568066	5.192918624	-2.391315523	0.020198629	0.87125001	-3.405863301

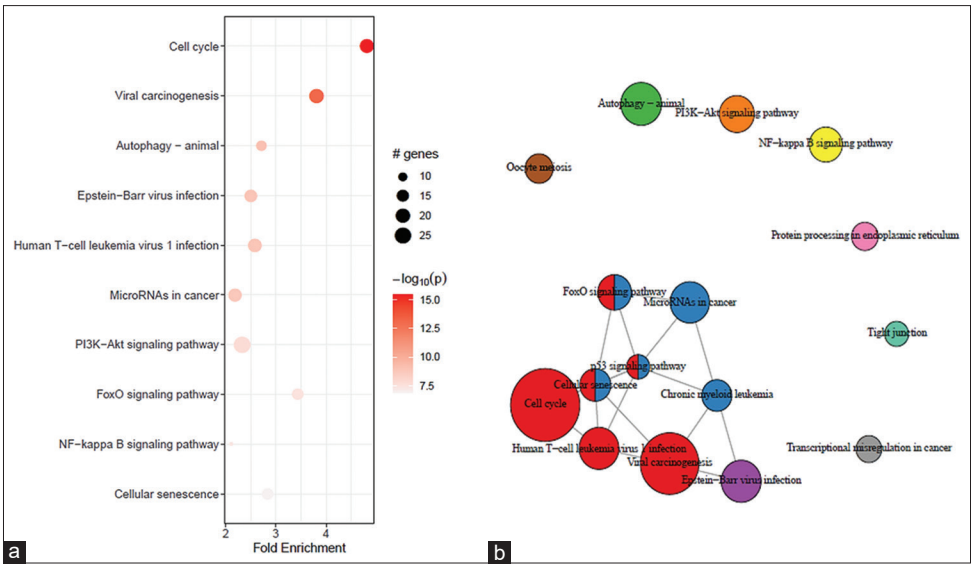

Figure 2: (a) The bubble chart of the KEGG pathway analysis of DEGs. (b) The clustering between the KEGG pathway enrichments based on the shared genes

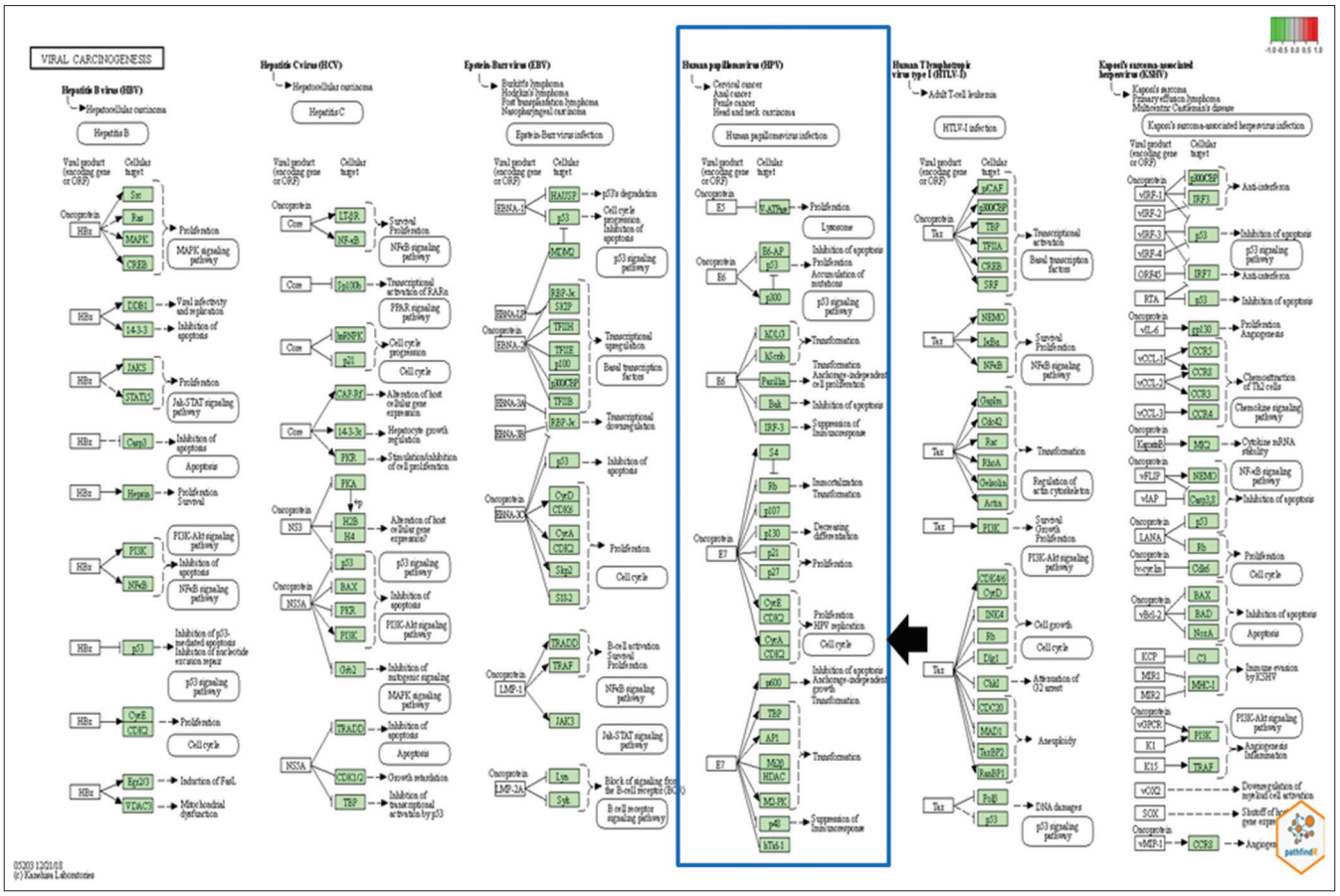

Figure 3: Viral carcinogenesis. The cell cycle involvement in the HPV carcinogenesis is demonstrated in the viral carcinogenesis pathways of different viruses

independence and mean connectivity are given in Figure 4b. Thirteen modules were identified, labeled with colors, and depicted in the dendrograms provided in Figure 4c. The clusters found during the clustering process are shown in different colors. There are color levels below the dendrogram, with the module displaying the integration phase. The gene expression profile's adjacency and correlation matrices were constructed to generate a

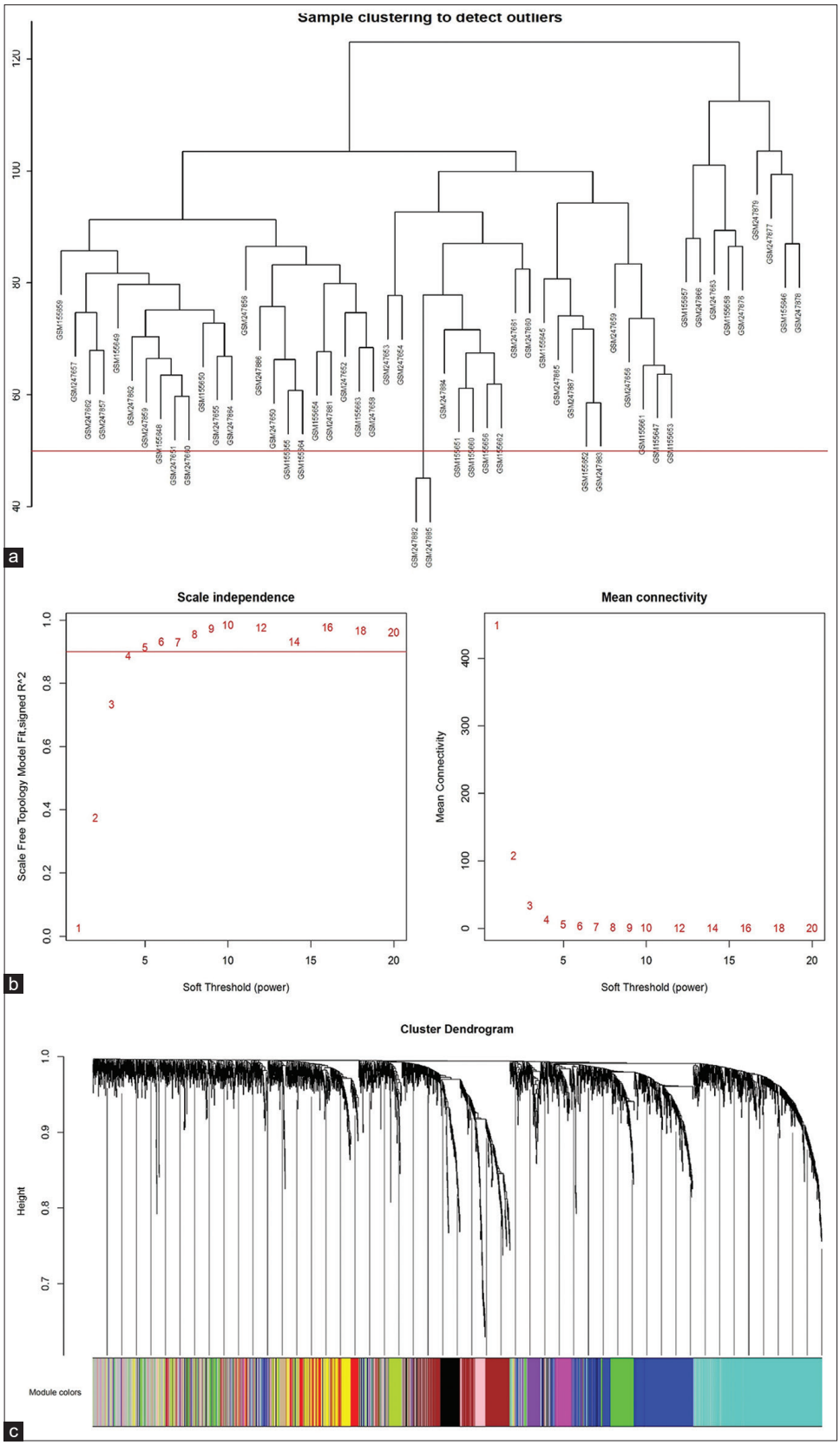

Figure 4: WGCNA analysis. (a) Sample clustering dendrogram and identification of outliers (the outliers were removed after identification). (b) The soft threshold selection. Scale-free topology fitting index R2 analysis (left) and mean connectivity for various soft threshold powers (right). The left panel's red line indicates that R2 = 4. (c) A clustering diagram of gene modules denoted by distinct colors

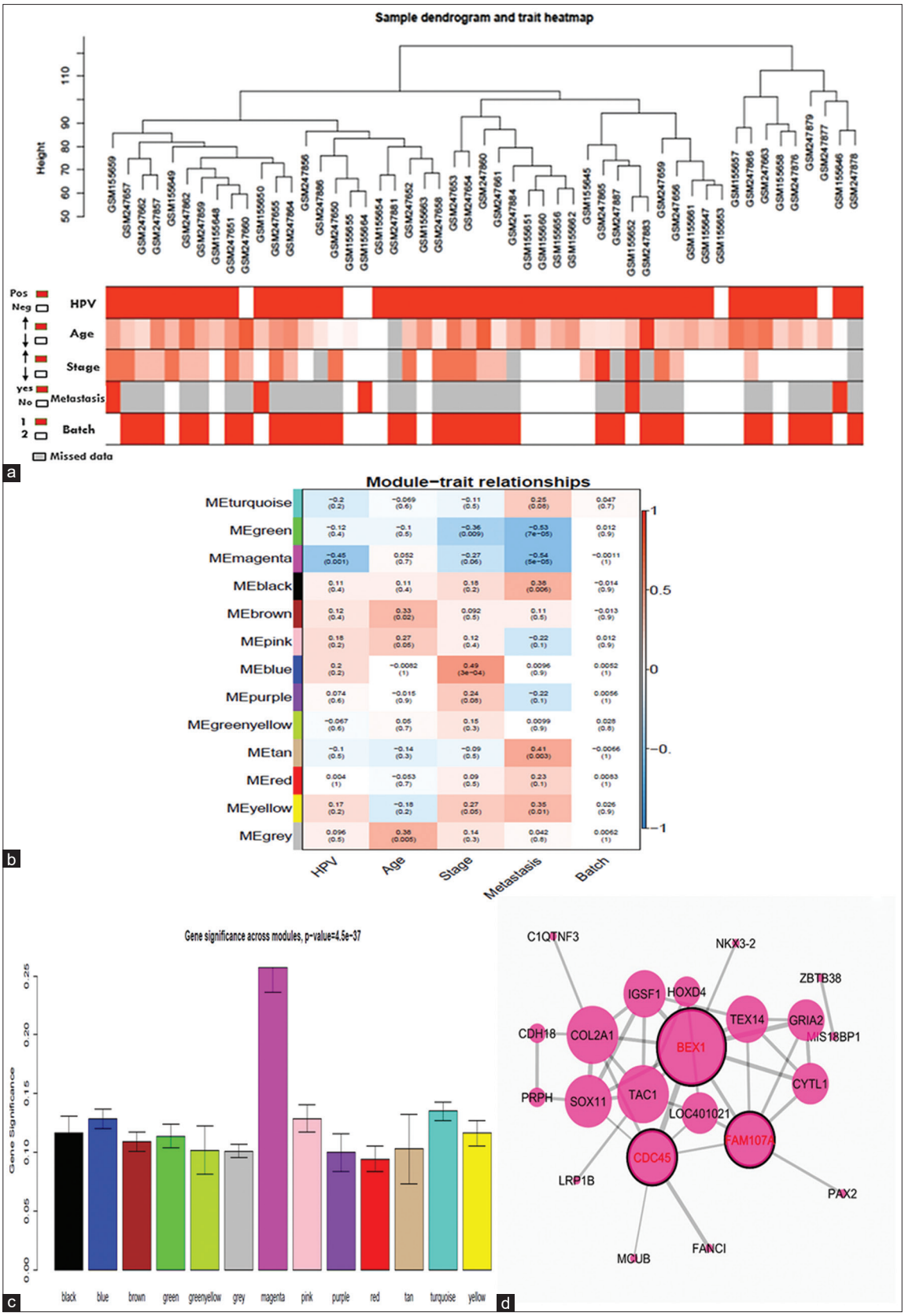

Figure 5: (a) Clinical trait heatmap and sample dendrogram. The sample dendrogram's threshold value is set at 100 to remove samples with considerable variability. (b) Module–trait relationship heatmap. Hierarchical clustering of module eigengenes that represent the clustering analysis's modules. The module is represented by the row, while the column represents the trait. The *P* values in the box show the correlation and *P* value. (c) The gene significance across the modules. The magenta module showed significant module–trait relationship among the other modules (*P* value = 4.5e-37). (d). *BEX1*, *CDC45*, and FAM107A identified the magenta module gene–gene interaction as the module hub genes

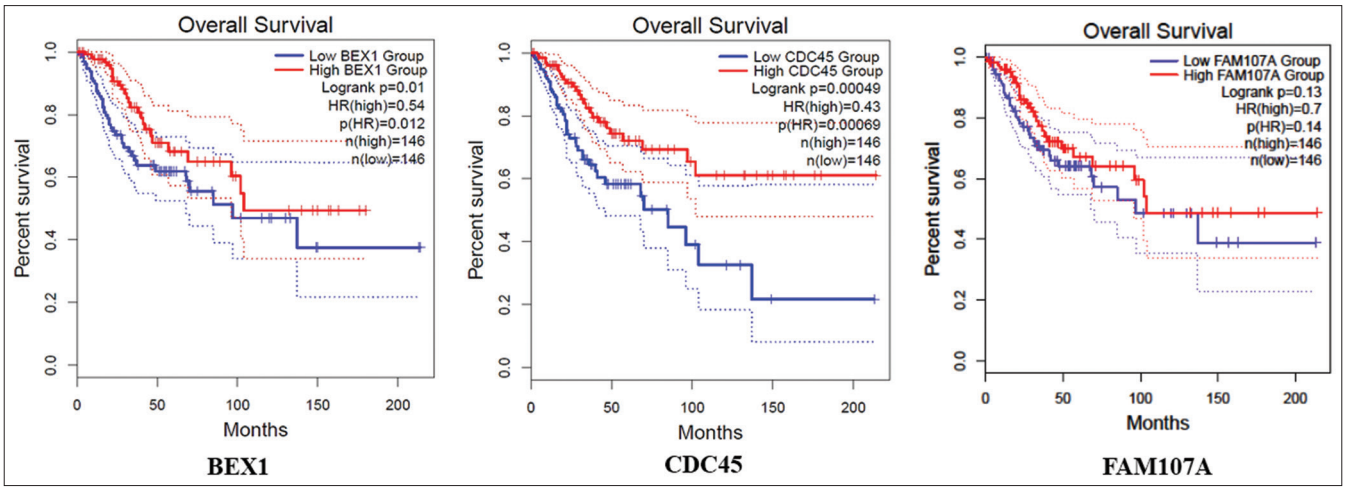

Figure 6: The relationship between the magenta module hub-gene expression and the clinical outcome in cervical cancer patients. The lower expression of *BEX1* (Logrank $P = 0.01$) and *CDC45* (Logrank $P = 0.00049$) exhibited significantly worse overall survival. The *GAPDH* gene was utilized to normalize data from targeted genes

topological overlap matrix (TOM), and the TOM type was considered as "unsigned".

Relating consensus modules to cervical cancer and identification of hub genes

The tables of module–trait relationships indicated the relationship between the clinical traits (HPV-positive or -negative, age, cervical cancer stages, metastasis, and batch in Figure 5a) and the consensus modules in each data set. Five relationship tables exhibit some degree of similarity. To explain further, the magenta module showed significant relations to HPV, cervical cancer stage, and metastasis. The magenta modules included 22 genes. The magenta module's hub genes were identified, including brain-expressed X-linked 1 (*BEX1*), Family with Sequence Similarity 107 Member A (*FAM107A*), and cell division cycle 45 (*CDC45*) [Figure 5b-d]. In addition, the *BEX1* and *FAM107A* expression levels decreased, and the *CDC45* expression level increased.

Survival analysis

The patient's overall survival rate and median survival time with altered expression of *BEX1*, *FAM107A*, and *CDC45* demonstrated that *BEX1* (Logrank $P = 0.01$) and *CDC45* (Logrank $P = 0.00049$) are associated with poor prognosis and overall survival of cervical cancer ($P < 0.05$) [Figure 6]. GEPIA is able to provide predictions on the survival rates of genes by using the RNA-seq data in TCGA.

Discussion

The infection of high-risk HPV is strongly linked to the development and progression of cervical cancer.[4,5] Additionally, growing data suggest that many DEGs are expressed by cancer cells.[27] In cancer cells, abnormal gene expression levels might potentially contribute to the dysregulation of cell signaling pathways by either blocking or activating the pathways.[28] Additionally, growing data suggest that many DEGs are expressed by cancer cells.[29] In cancer cells, abnormal gene expression levels might potentially contribute to the dysregulation of cell signaling pathways by either blocking or activating the pathways.[30] Notably, in the present study, 115 DEGs from both datasets are retrieved according to the given criterion. KEGG pathway enrichment analysis was used further to study these DEGs' relevance in HPV-associated cervical cancer. "Cell cycle," "Viral carcinogenesis," "Autophagy-animal," "Epstein-Barr virus infection," "Human T-cell leukemia virus 1 infection," and "MicroRNAs in cancer" were among the main pathways enriched by the majority of the DEGs. As is widely known, HPVs propagate by interfering with normal cell cycle regulation processes and increasing cell proliferation.[31] HPV also causes cell senescence in cervical cancer cells. Continuous proliferation and senescence cause DNA damage, resulting in neoplastic changes in the cervix.[32,33] Malignant transformation is also intricately tied to these processes, and the carcinogenic potential of papillomaviruses probably rests in their capacity to modify cell cycle checkpoints, resulting in the accumulation and propagation of genetic abnormalities.[34] In this regard, HPV and EBV are linked to 38% of all virus-associated malignancies.[35] De Lima *et al*.'s[36] latest meta-analysis indicated a 29% HPV/EBV co-infection rate in cervical cancer. They also discovered a link between EBV load and lesion grade (from CIN 1 to CIN 3 and invasive carcinoma), indicating that EBV may have a role in the development and progression of cervical cancer. The presence of EBV in the cervix may also hasten the integration of the HPV genome into the genome of the cervical cell, increasing the genomic instability of the infected cervical cells.[37]

Autophagy, a cellular process that removes damaged or dysfunctional components, plays a complex role in cervical cancer development. On one hand, autophagy functions as a defense mechanism by clearing infected cells and preventing

malignant transformation. However, autophagy can also promote HPV replication and survival, facilitating cancer cell progression and drug resistance while suppressing immune responses.[38] Of note, HPV infection upregulates several autophagy-related proteins in cervical cancer cells. For instance, the E6 and E7 oncoproteins produced by HPV infection are known to increase the expression of Beclin1, a critical regulator of autophagy initiation.[39] Therefore, modulating autophagy may hold promise as a potential therapeutic approach for cervical cancer, but it requires careful consideration of both its beneficial and harmful effects.[38] To clarify, targeting ATG9B and LAMP1, two genes that are overexpressed in HPV-associated cervical cancer, is a promising therapeutic strategy. Several inhibitors that block the function of these genes are currently being studied as potential treatments for HPV-induced cervical cancer.[40] Furthermore, the functions of miRNAs in HPV-associated cervical cancer are well understood.[41] In 2020, Babion *et al*.[42] evaluated the miRNA expression profile linked with HPV infection in eight distinct passages of HPV-transformed keratinocytes, reflecting various phases of cell transformation produced by HPV infection using micro-arrays. The most typical miRNAs verified by RT-qPCR were *miR-15b-5p*, *miR-100-5p*, *miR-103a-3p*, and *miR-125b-5p*, which were all shown to be elevated, whereas only *miR-221-5p* was found to be down-regulated. Another research linked the severity of HPV-16-infected women's intra-epithelial lesions to the expression of four miRNAs including *miR-16*, *miR-21*, *miR-34a*, and *miR-143*. Remarkably, compared to the HPV-negative group, *miR-21* expression rose dramatically, while *miR-143* expression declined.[43] It should be noted that the clustering between the crucial pathways based on the shared genes indicates that most of the genes are similar, which points to the significance of these DEGs in HPV-associated cervical cancer.

WGCNA is a co-expression network technique that is commonly utilized in cancer marker research. Although prior research studies used WGCNA to identify numerous prognostic indicators in cervical cancer, they primarily focused on DEGs across groups (HPV-positive and HPV-negative).[17] Despite this, the clinical profile of patients has not been considered. Furthermore, we investigated clinical indications that may be associated with cervical cancer patients. As a result, in this work, we first screened DEGs between normal and tumor tissues and then performed WGCNA while taking five clinical/technical aspects of the cervical cancer patient samples into account, including HPV positivity or negativity, age, cervical cancer stage, metastasis, and batch. Finally, a total of 13 modules were associated with these clinical traits. The magenta module is significantly related to HPV, cervical cancer stage, and metastasis. Only after a long-term infection may HPV cause low- and/or high-grade CIN, which can progress to cervical cancer.[44-46] The most frequent high-risk HPV strains are HPV16 and HPV18, which cause around 70% of cervical malignancies (50% HPV16, 20% HPV18).[47,48] Furthermore, Okonogi *et al*.[49] discovered that HPV genotype influenced the 5-year distant metastatic risk in cervical cancer, although research on HPV and cervical cancer metastasis is restricted.

On the other hand, the magenta module's hub genes were identified, including *BEX1*, *FAM107A* with decreased expression, and *CDC45* with increased expression. *FAM107A*, commonly referred to as down-regulated renal cell carcinoma gene 1 (*DRR1*), was identified by Tohoku University cDNA clone A on chromosome 3 (*TU3A*).[50,51] *FAM107A* is a protein-coding gene that produces a nuclear protein composed of 144 amino acids and a coiled-coil domain. As a result, through interacting with DNA and/or other proteins, *FAM107A* may influence gene expression. The expression of *FAM107A* is decreased in a number of different cancers, including neuroblastoma,[50] renal cell carcinoma,[51] lung cancer,[52] and laryngeal tumors. Furthermore, FAM107A has an important role in promoting tumor cell proliferation.[53] In this regard, our results demonstrated that *FAM107A* expression levels also decreased in cervical cancer, although *FAM107A* survival analysis results were not associated with any significant outcome.

In addition, the overall survival rate and median survival time of the patients with altered expression of *BEX1* and *CDC45* demonstrated that *BEX1* (Logrank $P = 0.01$) and *CDC45* (Logrank $P = 0.00049$) are associated with poor prognosis and overall survival of cervical cancer patients ($P < 0.05$). The human *BEX* family proteins are essential proteins in neuronal development and comprise five proteins (*BEX1-5*).[54] The first indication of *BEX1*, an intra-cellular signal transducer or regulator, was a reduction in expression in retinoic acid-treated F9 teratoma cells. *BEX1* has a role in axon regeneration,[55] and it also interacts with the p75 neurotrophing receptor (NTR) and helps to regulate the cell cycle.[56] Previous research has shown that proteins belonging to the BEX family are linked to a variety of different human cancers. Over-expression of BEX1 in breast cancer leads to a suppression of tumor cell apoptosis.[57,58] Additionally, it has been shown that the level of *BEX1* mRNA is elevated during the process of hepatocyte dedifferentiation. *BEX1* is regarded as a marker for the processes of hepatocyte differentiation and dedifferentiation as well as tumor development.[59] *BEX1* expression in hepatocellular carcinoma cell lines was substantially higher than in normal hepatocyte cell lines, enhancing cell proliferation.[60] Additionally, *BEX1* serves as a chemotherapy resistance marker.[61] It has been shown that over-expressed *BEX1* has a role in the development of neuroendocrine-specific malignancies.[62] Conversely, the expression of *BEX1* was inhibited in malignant glioma, both in glioma cell lines and in primary patient samples.[63] Therefore, *BEX1* may regulate the biological processes of neoplasms in two distinct ways.

On the other hand, *CDC45* is one of the proteins that are necessary for the initiation, development, and regulation of the DNA replication process. It has been discovered that *CDC45*,

mini-chromosome maintenance protein complex (MCM), and Go-Ichi-Ni-San (GINS) create a "super complex" that is the major component of eukaryotic replicons and contains helicase activity.[64] Throughout the DNA replication process, it attaches to DNA molecules and unfolds double-stranded DNA to generate a replication fork formation.[65] According to earlier research, *CDC45* may be an antigen involved in the proliferation process and may also contribute to the advancement of malignant tumors.[66] Furthermore, studies have discovered that CDC45 is one of the myc gene's target genes, and that it plays a key role in myc-dependent DNA replication stress as well as regulating the replication origin activation rate.[67,68] In particular, the "recapitulates all c-myc-induced replication and damage phenotypes" may be seen as a result of the over-expression of *CDC45*.[69] These considerations indicate a significant function for *CDC45* in carcinogenesis. In this regard, He *et al*.[70] revealed that *CDC45* expression increased and may be a possible biomarker related to cervical cancer prognosis. Similarly, our results demonstrated over-expression of *CDC45* in cervical cancer, and based on the survival analysis, *CDC45* was identified as a prognostic factor in cervical cancer.

Limitations

Our study has two limitations: It exclusively examines publicly available databases, which might not provide a thorough comprehension of the subject of investigation and lacks direct experimental validation, potentially impacting the generalizability and applicability of the results. Nevertheless, the study still offers valuable perspectives by utilizing the abundance of data in publicly available databases. This methodology allows for the exploration of extensive datasets and the detection of intricate patterns that are not readily noticeable through smaller experiments. To point out, bioinformatics analyses offer a comprehensive and impartial perspective on the molecular alterations associated with cancer, generating large-scale datasets and enabling the identification of complex patterns and connections that may not be readily discerned through traditional laboratory experiments alone. Traditional laboratory experiments can be labor-intensive and expensive and require specialized equipment. However, bioinformatics analyses leverage openly available datasets and software, making it more accessible and cost-effective. Furthermore, the ability to efficiently analyze extensive datasets and conduct intricate statistical analyses using bioinformatics tools allows for the rapid discovery of novel perspectives and hypotheses, thereby facilitating advancements in cancer research. Considering the potential importance of the detected hub genes, we recommend conducting additional in-depth wet lab research to determine their impact on biological mechanisms of papillomavirus-associated cervical cancer. We foresee that ongoing research in this field will provide valuable knowledge about the fundamental mechanisms of cervical cancer and guide future approaches to effective treatment.

Conclusion

In conclusion, the innovation of our work lies in the identification of essential genes associated with the multi-step process of cervical carcinogenesis. To enumerate, we identified the DEGs related to HPV-associated cervical cancer. We enriched the DEGs to discover the pathways these genes potentially affected. Notably, pathway clustering revealed the pathways with the highest shared DEGs, which are beneficial trajectories in HPV-associated cervical cancer. The magenta module had the most robust relationship with cervical cancer phenotypes, according to the WGCNA study. In addition, the potential of *BEX1* and *CDC45* magenta module hub genes as the prognostic factors in cervical cancer was identified, and their direct relationship with the patient's survival was assessed.

Financial support and sponsorship

This work was supported in part by Shahrekord University.

Conflicts of interest

There are no conflicts of interest.

References

1. Arbyn M, Weiderpass E, Bruni L, de Sanjosé S, Saraiya M, Ferlay J, Bray F. Estimates of incidence and mortality of cervical cancer in 2018: a worldwide analysis. Lancet Glob Health. 2020;8:e191-e203.
2. Ferlay J, Colombet M, Soerjomataram I, Mathers C, Parkin DM, Piñeros M, *et al*. Estimating the global cancer incidence and mortality in 2018: GLOBOCAN sources and methods. Int J cancer 2019;144:1941–53.
3. Zhang S, Xu H, Zhang L, Qiao Y. Cervical cancer: Epidemiology, risk factors and screening. Chin J Cancer Res 2020;32:720-8.
4. Schiffman M, Doorbar J, Wentzensen N, De Sanjosé S, Fakhry C, Monk BJ, Stanley MA, Franceschi S. Carcinogenic human papillomavirus infection. Nat Rev Dis Prim. 2016;2:1–20.
5. Walboomers JMM, Jacobs MV, Manos MM, Bosch FX, Kummer JA, Shah K V, Snijders P J, Peto J, Meijer C J, Muñoz N. Human papillomavirus is a necessary cause of invasive cervical cancer worldwide. J Pathol. 1999;189:12–9.
6. Yeo-Teh NSL, Ito Y, Jha S. High-risk human papillomaviral oncogenes E6 and E7 target key cellular pathways to achieve oncogenesis. Int J Mol Sci 2018;19:1706.
7. Kessler TA. Cervical cancer: Prevention and early detection. In: Seminars in Oncology Nursing. Elsevier; 2017. p. 172–83.
8. Gadducci A, Tana R, Cosio S, Cionini L. Treatment options in recurrent cervical cancer. Oncol Lett. Spandidos Publications; 2010;1:3–11.
9. Serkies K, Jassem J. Systemic therapy for cervical carcinoma–current status. Chinese J Cancer Res 2018;30:209.
10. Hou P, Hsieh C, Wei M, Hsiao S, Shueng P. Differences in treatment outcomes and prognosis between elderly and younger patients receiving definitive radiotherapy for cervical cancer. Int J Environ Res Public Health 2020;17:4510.
11. Basu P, Taghavi K, Hu S-Y, Mogri S, Joshi S. Management of cervical premalignant lesions. Curr Probl Cancer. 2018;42:129–36.
12. Ma S, Wang J, Han Y, Guo F, Chen C, Chen X, *et al*. Platinum single-agent vs. platinum-based doublet agent concurrent chemoradiotherapy for locally advanced cervical cancer: A meta-analysis of randomized controlled trials. Gynecol Oncol 2019;154:246–52.
13. Yang J, Huang T, Petralia F, Long Q, Zhang B, Argmann C, Zhao Y, Mobbs CV, Schadt EE, Zhu J, Tu Z; GTEx Consortium. Synchronized age-related gene expression changes across multiple tissues in human and the link to complex diseases. Sci Rep. 2015 Oct 19;5:15145.
14. Cui D, Yuan W, Chen C, Han R. Identification of colorectal cancer-

associated macrophage biomarkers by integrated bioinformatic analysis. Int J Clin Exp Pathol. 2021 ;14:1-8.
15. Xu X, Long H, Xi B, Ji B, Li Z, Dang Y, *et al*. Molecular network-based drug prediction in thyroid cancer. Int J Mol Sci 2019;20:263.
16. Liu C, Wei D, Xiang J, Ren F, Huang L, Lang J, *et al*. An improved anticancer drug-response prediction based on an ensemble method integrating matrix completion and ridge regression. Mol Ther Acids 2020;21:676–86.
17. Liu J, Nie S, Gao M, Jiang Y, Wan Y, Ma X, *et al*. Identification of EPHX2 and RMI2 as two novel key genes in cervical squamous cell carcinoma by an integrated bioinformatic analysis. J Cell Physiol 2019;234:21260–73.
18. Balasubramaniam SD, Balakrishnan V, Oon CE, Kaur G. Key molecular events in cervical cancer development. Medicina (Kaunas) 2019;55:384.
19. Zhou XL, Wang M. Expression levels of survivin, Bcl-2, and KAI1 proteins in cervical cancer and their correlation with metastasis. Genet Mol Res. 2015;14:17059–67.
20. Langfelder P, Horvath S. WGCNA: an R package for weighted correlation network analysis. BMC Bioinformatics. 2008;9:1–13.
21. Gautier L, Cope L, Bolstad BM, Irizarry RA. affy–analysis of Affymetrix GeneChip data at the probe level. Bioinformatics. Oxford University Press. 2004;20:307–15.
22. Xie Y, Wu H, Hu W, Zhang H, Li A, Zhang Z, *et al*. Identification of hub genes of lung adenocarcinoma based on weighted gene Co-expression network in Chinese population. Pathol Oncol Res 2022;28:1610455.
23. Kanehisa M, Furumichi M, Tanabe M, Sato Y, Morishima K. KEGG: New perspectives on genomes, pathways, diseases and drugs. Nucleic Acids Res 2017;45:D353–61.
24. Ulgen E, Ozisik O, Sezerman OU. pathfindR: An R package for comprehensive identification of enriched pathways in omics data through active subnetworks. Front Genet 2019;10:858.
25. Sipko van Dam, Urmo Võsa, Adriaan van der Graaf, Lude Franke, João Pedro de Magalhães, Gene co-expression analysis for functional classification and gene–disease predictions, Briefings in Bioinformatics, Volume 19, Issue 4, July 2018, Pages 575–592.
26. Ovens K, Eames BF, McQuillan I. Comparative analyses of gene co-expression networks: Implementations and applications in the study of evolution. Front Genet. 2021;12:695399.
27. Van Wieringen WN, Van der Vaart AW. Transcriptomic heterogeneity in cancer as a consequence of dysregulation of the gene–gene interaction network. Bull Math Biol. 2015;77:1768–86.
28. Vogelstein B, Kinzler KW. Cancer genes and the pathways they control. Nat Med. 2004;10:789–99.
29. Jiang M, Milner J. Selective silencing of viral gene expression in HPV-positive human cervical carcinoma cells treated with siRNA, a primer of RNA interference. Oncogene. 2002;21:6041–8.
30. Saleh T, Khasawneh AI, Himsawi N, Abu-Raideh J, Ejeilat V, Elshazly AM, *et al*. Senolytic therapy: A potential approach for the elimination of oncogene-induced senescent HPV-positive cells. Int J Mol Sci 2022;23:15512.
31. Fernandes JV, Fernandes TAADM, de Azevedo JCV, Cobucci RNO, de Carvalho MGF, Andrade VS, *et al*. Link between chronic inflammation and human papillomavirus-induced carcinogenesis (Review). Oncol Lett 2015;9:1015–26.
32. Vats A, Trejo-Cerro O, Thomas M, Banks L. Human papillomavirus E6 and E7: What remains? Tumour Virus Res 2021;11:200213.
33. Shi Y, Peng S-L, Yang L-F, Chen X, Tao Y-G, Cao Y. Co-infection of Epstein-Barr virus and human papillomavirus in human tumorigenesis. Chin J Cancer 2016;35:1–9.
34. de Lima MAP, Neto PJN, Lima LPM, Júnior JG, Junior AGT, Teodoro IPP, *et al*. Association between Epstein-Barr virus (EBV) and cervical carcinoma: A meta-analysis. Gynecol Oncol 2018;148:317–28.
35. Kahla S, Oueslati S, Achour M, Kochbati L, Chanoufi MB, Maalej M, Oueslati R. Correlation between ebv co-infection and HPV16 genome integrity in Tunisian cervical cancer patients. Brazilian J Microbiol. 2012;43:744–53.
36. Wu L, Shen B, Li J, Zhang H, Zhang K, Yang Y, *et al*. STAT3 exerts pro-tumor and anti-autophagy roles in cervical cancer. Diagn Pathol 2022;17:182.
37. Lagunas-Martínez A, Madrid-Marina V, Gómez-Cerón C, Deas J, Peralta-Zaragoza O. The autophagy process in cervical carcinogenesis: Role of non-coding-RNAs, molecular mechanisms, and therapeutic targets. Cells 2022;11:1323.
38. Tingting C, Shizhou Y, Songfa Z, Junfen X, Weiguo L, Xiaodong C, *et al*. Human papillomavirus 16E6/E7 activates autophagy via Atg9B and LAMP1 in cervical cancer cells. Cancer Med 2019;8:4404–16.
39. Bañuelos-Villegas EG, Pérez-yPérez MF, Alvarez-Salas LM. Cervical cancer, papillomavirus, and miRNA dysfunction. Front Mol Biosci 2021;8:758337.
40. Babion I, Miok V, Jaspers A, Huseinovic A, Steenbergen RDM, van Wieringen WN, *et al*. Identification of deregulated pathways, key regulators, and novel miRNA-mRNA interactions in HPV-mediated transformation. Cancers (Basel) 2020;12:12030700.
41. Norouzi S, Farhadi A, Farzadfard E, Akbarzade-Jahromi M, Ahmadzadeh N, Nasiri M, *et al*. MicroRNAs expression changes coincide with low or high grade of squamous intraepithelial lesion infected by HPV-16. Gene Rep 2021;23:101186.
42. Östör AG. Studies on 200 cases of early squamous cell carcinoma of the cervix. Int J Gynecol Pathol. LWW; 1993;12:193–207.
43. Ermel A, Shew ML, Imburgia TM, Brown M, Qadadri B, Tong Y, *et al*. Redetection of human papillomavirus type 16 infections of the cervix in mid-adult life. Papillomavirus Res 2018;5:75–9.
44. Tommasino M. The Human Papillomavirus Family and Its role in Carcinogenesis. In: Seminars in Cancer Biology. Elsevier; 2014. p. 13–21.
45. Gupte S, Parthasarathy S, Arora P, Ozalkar S, Jangam S, Rajwade K, Nikam P, Shah S. A Rapid, Sensitive and Type-Specific Detection of High-Risk HPV-16 and HPV-18. J Obstet Gynaecol India. 2023 Oct;73(5):440-444.
46. Nakowong P, Chatchawal P, Chaibun T, Boonapatcharoen N, Promptmas C, Buajeeb W, Lee SY, Jearanaikoon P, Lertanantawong B. Detection of high-risk HPV 16 genotypes in cervical cancers using isothermal DNA amplification with electrochemical genosensor. Talanta. 2023 Nov 28;269:125495.
47. Okonogi N, Kobayashi D, Suga T, Imai T, Wakatsuki M, Ohno T, *et al*. Human papillomavirus genotype affects metastatic rate following radiotherapy in patients with uterine cervical cancer. Oncol Lett 2018;15:459–66.
48. Mu P, Akashi T, Lu F, Kishida S, Kadomatsu K. A novel nuclear complex of DRR1, F-actin and COMMD1 involved in NF-κB degradation and cell growth suppression in neuroblastoma. Oncogene. 2017;36:5745-5756.
49. Yamato T, Orikasa K, Fukushige S, Orikasa S, Horii A. Isolation and characterization of the novel gene, TU3A, in a commonly deleted region on 3p14.3-->p14.2 in renal cell carcinoma. Cytogenet Cell Genet. 1999;87:291-5.
50. Yan D, Chen Y. Tumor mutation burden (TMB)-associated signature constructed to predict survival of lung squamous cell carcinoma patients. Sci Rep 2021;11:9020.
51. Kiwerska K, Szaumkessel M, Paczkowska J, Bodnar M, Byzia E, Kowal E, *et al*. Combined deletion and DNA methylation result in silencing of FAM107A gene in laryngeal tumors. Sci Rep 2017;7:5386.
52. Kazi JU, Kabir NN, Rönnstrand L. Brain-Expressed X-linked (BEX) proteins in human cancers. Biochim Biophys Acta Rev Cancer 2015;1856:226–33.
53. Khazaei MR, Halfter H, Karimzadeh F, Koo JH, Margolis FL, Young P. Bex1 is involved in the regeneration of axons after injury. J Neurochem. 2010;115:910–20.
54. Vilar M, Murillo-Carretero M, Mira H, Magnusson K, Besset V, Ibáñez CF. Bex1, a novel interactor of the p75 neurotrophin receptor, links neurotrophin signaling to the cell cycle. EMBO J. John Wiley & Sons, Ltd Chichester, UK; 2006;25:1219–30.
55. Naderi A, Teschendorff AE, Beigel J, Cariati M, Ellis IO, Brenton JD, Caldas C. BEX2 is overexpressed in a subset of primary breast cancers and mediates nerve growth factor/nuclear factor-κB inhibition of apoptosis in breast cancer cell lines. Cancer Res. 2007;67:6725–36.
56. Naderi A, Liu J, Bennett IC. BEX2 regulates mitochondrial apoptosis and G1 cell cycle in breast cancer. Int J cancer. 2010;126:1596–610.
57. Braeuning A, Jaworski M, Schwarz M, Köhle C. Rex3 (reduced in expression 3) as a new tumor marker in mouse hepatocarcinogenesis.

Toxicology. 2006;227:127–35.
58. Sagawa H, Naiki-Ito A, Kato H, Naiki T, Yamashita Y, Suzuki S, *et al*. Connexin 32 and luteolin play protective roles in non-alcoholic steatohepatitis development and its related hepatocarcinogenesis in rats. Carcinogenesis 2015;36:1539–49.
59. De Ronde JJ, Lips EH, Mulder L, Vincent AD, Wesseling J, Nieuwland M, *et al*. SERPINA6, BEX1, AGTR1, SLC26A3, and LAPTM4B are markers of resistance to neoadjuvant chemotherapy in HER2-negative breast cancer. Breast Cancer Res Treat 2013;137:213–23.
60. Doi T, Ogawa H, Tanaka Y, Hayashi Y, Maniwa Y. Bex1 significantly contributes to the proliferation and invasiveness of malignant tumor cells. Oncol Lett 2020;20:362.
61. Foltz G, Ryu G-Y, Yoon J-G, Nelson T, Fahey J, Frakes A, Lee H, Field L, Zander K, Sibenaller Z, Ryken TC, Vibhakar R, Hood L, Madan A. Genome-wide analysis of epigenetic silencing identifies BEX1 and BEX2 as candidate tumor suppressor genes in malignant glioma. Cancer Res. 2006;66:6665–74
62. Masai H, You Z, Arai K. Control of DNA replication: regulation and activation of eukaryotic replicative helicase, MCM. IUBMB Life. 2005;57:323–35.
63. Simon AC, Sannino V, Costanzo V, Pellegrini L. Structure of human Cdc45 and implications for CMG helicase function. Nat Commun 2016;7:11638.
64. He Z, Wang X, Yang Z, Jiang Y, Li L, Wang X, Song Z, Wang X, Wan J, Jiang S, Zhang N, Cui R. Expression and prognosis of CDC45 in cervical cancer based on the GEO database. PeerJ. 2021 Sep 3;9:e12114.
65. Nepon-Sixt BS, Bryant VL, Alexandrow MG. Myc-driven chromatin accessibility regulates Cdc45 assembly into CMG helicases. Commun Biol. 2019;2:1–15.
66. Srinivasan S V, Dominguez-Sola D, Wang LC, Hyrien O, Gautier J. Cdc45 is a critical effector of myc-dependent DNA replication stress. Cell Rep. 2013;3:1629–39.
67. Reed DR, Alexandrow MG. Myc and the Replicative CMG Helicase: The Creation and Destruction of Cancer: Myc Over-Activation of CMG Helicases Drives Tumorigenesis and Creates a Vulnerability in CMGs for Therapeutic Intervention. Bioessays 2020;42: e1900218.
68. He Z, Wang X, Yang Z, Jiang Y, Li L, Wang X, *et al*. Expression and prognosis of CDC45 in cervical cancer based on the GEO database. PeerJ 2021;9:e12114.
69. Scotto L, Narayan G, Nandula SV, Arias-Pulido H, Subramaniyam S, Schneider A, *et al*. Identification of copy number gain and overexpressed genes on chromosome arm 20q by an integrative genomic approach in cervical cancer: Potential role in progression. Genes Chromosom Cancer 2008;47:755–65.
70. Pyeon D, Newton MA, Lambert PF, Boon JA Den, Marsit CJ, Woodworth CD, *et al*. Fundamental differences in cell cycle deregulation in human papillomavirus-positive and human papillomavirus-negative head/neck and cervical cancers. Cancer Res 2007;67:4605–19.

Table S1: 115 DEGs of HPV-associated cervical cancer

ID	logFC	AveExpr	*t*	*P*	adj. *P*	*B*
AIM1	1.074147	10.08248	3.383018	0.001319	0.706486	-1.94717
ALDH3B2	1.006923	5.821987	2.33709	0.023063	0.87125	-3.47567
AMIGO2	-1.38945	7.740644	-2.10873	0.039488	0.88331	-3.75621
ANXA10	-1.59857	5.192919	-2.39132	0.020199	0.87125	-3.40586
APOBEC3B	1.398207	8.45479	2.41551	0.019027	0.87125	-3.37433
AQP3	1.755985	9.585711	2.408208	0.019374	0.87125	-3.38387
ARMCX1	-1.92488	6.132086	-3.67404	0.000538	0.640595	-1.4667
ASXL3	-1.00309	4.591111	-2.54656	0.013677	0.87125	-3.19959
ATP1A2	-1.14959	4.149151	-3.4149	0.001198	0.695686	-1.89547
BCHE	-1.1053	4.208793	-3.00107	0.004023	0.844751	-2.54577
BEX1	-1.13167	6.00612	-3.29307	0.001727	0.706486	-2.09167
BEX4	-1.36963	6.65742	-2.44166	0.017829	0.87125	-3.33999
C3	-1.52869	9.064344	-2.29758	0.025373	0.87125	-3.52578
CCNA1	-1.19489	5.692084	-2.51792	0.014714	0.87125	-3.23833
CCND1	-1.38661	6.630506	-3.09651	0.003066	0.804842	-2.4
CCND2	-1.16669	6.579516	-3.08106	0.003205	0.804842	-2.42378
CD52	1.351236	7.035058	2.428877	0.018406	0.87125	-3.35682
CD79B	1.006829	4.821491	2.592419	0.012155	0.87125	-3.13689
CDC45	1.093732	7.082903	2.228024	0.029943	0.87125	-3.61242
CDCA8	1.138421	8.467276	2.497577	0.015493	0.87125	-3.26567
CDH13	-2.25219	5.382494	-3.77544	0.00039	0.578434	-1.29513
CDKN2B	1.091656	4.150298	2.063349	0.043762	0.88331	-3.80926
CDKN2C	1.259212	7.974064	3.071874	0.003291	0.804842	-2.43789
CEACAM5	1.185924	7.892701	2.549555	0.013573	0.87125	-3.19551
CEP295	-1.07113	4.408704	-2.36846	0.021365	0.87125	-3.43544
CHRDL1	-1.35573	5.363282	-3.82081	0.000338	0.578434	-1.21774
CLU	-1.07226	6.895433	-2.02432	0.047753	0.88331	-3.85415
COL2A1	-1.14713	4.480598	-2.87604	0.0057	0.87125	-2.73252
CYTL1	-1.89299	4.244747	-3.46308	0.001035	0.695686	-1.8169
DACH1	-1.05512	4.149112	-2.60926	0.011636	0.87125	-3.11367
DLK1	-1.05369	5.019635	-2.14875	0.036025	0.88331	-3.70866
DUSP6	-1.37543	7.737265	-2.39	0.020264	0.87125	-3.40757
EHF	1.615501	7.507107	2.609951	0.011615	0.87125	-3.11272
ELF3	1.038059	9.172477	2.525663	0.014427	0.87125	-3.22789
EPHX3	1.597598	7.869302	2.202898	0.031765	0.87125	-3.64322
EYA2	1.26469	8.176101	2.022669	0.047928	0.88331	-3.85604
FAM107A	-1.15944	5.321467	-2.85984	0.005959	0.87125	-2.75634
FAM110B	-1.2604	4.2267	-2.96933	0.004399	0.844751	-2.59364
FAM169A	-1.4121	4.19548	-2.93513	0.00484	0.844751	-2.64487
FBN2	-1.15807	5.420929	-2.47202	0.016524	0.87125	-3.29979
FBXO17	-1.09667	4.51723	-2.75102	0.008004	0.87125	-2.91419
FRRS1L	-1.36822	4.127011	-2.93697	0.004815	0.844751	-2.64213
FST	-1.22107	7.711789	-2.15706	0.03534	0.88331	-3.6987
FZD2	-1.47099	6.0517	-3.12187	0.002851	0.804842	-2.36083
FZD7	-1.15485	6.444111	-2.32134	0.023961	0.87125	-3.49572
GPM6A	-1.13367	3.646323	-3.5533	0.000784	0.641834	-1.66831
GPSM2	1.045921	8.368603	2.286384	0.026064	0.87125	-3.53987
GPX3	-1.45925	8.096977	-2.48057	0.016172	0.87125	-3.28841
GRIA2	-1.10894	2.988487	-3.25996	0.001905	0.733597	-2.14434
GSPT2	-1.18578	5.777751	-2.27699	0.026657	0.87125	-3.55164
HIST1H2AE	-1.24883	5.635479	-2.18265	0.033303	0.876958	-3.66784
HOXD4	-1.15666	6.815015	-2.63989	0.010743	0.87125	-3.07118
HTRA1	-1.07633	9.549259	-2.57679	0.012655	0.87125	-3.15834
IGSF1	-1.35355	5.846481	-3.19132	0.00233	0.780056	-2.2526
IL13RA2	-1.16048	4.367197	-2.11924	0.038551	0.88331	-3.74378
IRS1	-1.04375	7.291966	-2.08478	0.041696	0.88331	-3.78432
IRS2	-1.32124	8.360021	-2.61873	0.011353	0.87125	-3.10057
ISG20	1.155749	8.134214	2.161854	0.034951	0.88331	-3.69294

Contd...

Table S1: Contd...

ID	logFC	AveExpr	*t*	*P*	adj. *P*	*B*
JMJD7	1.314984	6.568228	2.133647	0.037299	0.88331	-3.72669
KCNJ16	-1.45414	4.732335	-2.45565	0.017217	0.87125	-3.32152
KCTD12	-1.04039	7.880285	-2.18548	0.033084	0.876731	-3.66441
KRT15	3.393498	10.75089	2.83276	0.006417	0.87125	-2.796
LALBA	-1.01379	4.412143	-3.29957	0.001694	0.706486	-2.0813
LDLRAP1	1.177026	8.09425	3.324238	0.001574	0.706486	-2.04183
LIMCH1	-1.07792	6.368078	-2.12239	0.038274	0.88331	-3.74005
LOC100506718	-1.60137	6.335646	-3.11574	0.002901	0.804842	-2.37031
LOC202181	-1.00714	4.734826	-2.243	0.028902	0.87125	-3.59394
MAP3K6	1.386721	7.267793	3.620085	0.000637	0.641834	-1.55717
MCM5	1.130396	8.954143	3.065075	0.003355	0.804842	-2.44831
MCUB	1.008121	8.856067	2.572171	0.012807	0.87125	-3.16467
MFAP4	-1.24451	5.628312	-2.09682	0.040573	0.88331	-3.77022
MIA	-1.17683	5.586853	-2.5954	0.012062	0.87125	-3.13279
MIR1908	-1.1676	8.056715	-2.64407	0.010626	0.87125	-3.06535
MPDZ	-1.13175	6.572449	-2.64136	0.010702	0.87125	-3.06912
MYO6	1.031134	7.391995	2.496989	0.015516	0.87125	-3.26646
NAALAD2	-1.02197	3.170201	-2.63836	0.010786	0.87125	-3.07331
NAP1L2	-1.66128	4.261196	-4.2821	7.39E-05	0.578434	-0.41226
NID1	-1.13682	6.766553	-2.7194	0.00871	0.87125	-2.9593
NKG7	1.219313	5.607442	2.024425	0.047742	0.88331	-3.85403
NPL	1.292535	7.141271	2.799777	0.007019	0.87125	-2.84396
NPTX2	-1.31017	5.979449	-2.33403	0.023236	0.87125	-3.47958
NR2E1	-1.16637	4.338757	-2.51241	0.014921	0.87125	-3.24576
NUPR1	1.35072	9.18664	2.628094	0.011079	0.87125	-3.08758
P2RX7	1.021708	5.179146	2.170263	0.034276	0.88331	-3.68281
PAX2	-1.02428	5.27348	-2.4817	0.016126	0.87125	-3.28691
PENK	-1.06639	5.787454	-2.96105	0.004502	0.844751	-2.60607
PLCB4	-1.10561	4.611086	-2.29125	0.025762	0.87125	-3.53375
PNMAL1	-1.66417	5.424176	-3.46099	0.001042	0.695686	-1.82032
PPP1R1A	-1.10314	3.283623	-3.24051	0.002017	0.733597	-2.17515
PTPRM	-1.31446	6.918241	-2.67178	0.00988	0.87125	-3.02657
RORA	1.233271	6.41574	2.579971	0.012552	0.87125	-3.15399
S100A8	1.43944	10.38959	2.104987	0.039826	0.88331	-3.76062
SACS	-1.01677	5.748076	-2.24233	0.028948	0.87125	-3.59477
SALL1	-1.00707	3.89698	-2.11386	0.039028	0.88331	-3.75015
SCUBE2	-1.05843	5.996673	-2.20842	0.031357	0.87125	-3.63648
SDC1	1.14971	11.08418	2.838021	0.006326	0.87125	-2.78831
SLC16A2	-1.01334	6.537062	-2.33824	0.022999	0.87125	-3.4742
SLC7A11	-1.11539	6.142438	-2.15721	0.035328	0.88331	-3.69852
SOX11	-1.25716	4.247944	-2.95095	0.004631	0.844751	-2.62121
SPARCL1	-1.19946	9.315417	-2.02245	0.047951	0.88331	-3.85628
SPINT1	1.08463	8.7344	3.175115	0.002443	0.780056	-2.27797
SPRY1	-1.20804	7.294399	-3.55942	0.00077	0.641834	-1.65817
SUCLA2	-1.0237	8.146297	-3.15564	0.002585	0.787077	-2.30836
SV2A	-1.04655	5.590412	-2.13081	0.037543	0.88331	-3.73006
SYNGR3	2.114242	7.41914	3.676141	0.000535	0.640595	-1.46317
TENM1	-1.4867	3.556463	-2.52734	0.014365	0.87125	-3.22562
TFPI2	-1.4007	3.81437	-2.46573	0.016787	0.87125	-3.30815
TRAF2	1.195507	6.904384	3.917692	0.000247	0.578434	-1.05125
TTC9	1.107535	6.316589	2.108041	0.03955	0.88331	-3.75702
TUSC3	-1.34082	6.977978	-2.05167	0.044924	0.88331	-3.82276
VAMP8	1.050173	10.35731	2.583427	0.012441	0.87125	-3.14924
WNT4	1.342326	5.717302	2.039559	0.046159	0.88331	-3.83671
WNT7B	1.217968	5.148196	4.018664	0.000178	0.578434	-0.8761
ZBTB10	-1.18494	4.279242	-2.23941	0.029149	0.87125	-3.59838
ZNF813	-1.00836	4.49645	-2.02646	0.047526	0.88331	-3.85171